

# Instanton Contribution to the Pion Electro-Magnetic Formfactor at $Q^2 > 1 \text{ GeV}^2$

P. Faccioli, A. Schwenk, and E.V. Shuryak

Department of Physics and Astronomy, State University of New York, Stony Brook, N.Y. 11794-3800

(Dated: October 28, 2018)

We study the effects of instantons on the charged pion electro-magnetic formfactor at intermediate momenta. In the Single Instanton Approximation (SIA), we predict the pion formfactor in the kinematic region  $Q^2 = 2 - 15 \text{ GeV}^2$ . By developing the calculation in a mixed time-momentum representation, it is possible to maximally reduce the model dependence and to calculate the formfactor directly. We find the intriguing result that the SIA calculation coincides with the vector dominance monopole form, up to surprisingly high momentum transfer  $Q^2 \sim 10 \text{ GeV}^2$ . This suggests that vector dominance for the pion holds beyond low energy nuclear physics.

PACS numbers: 13.40.Gp; 12.38.Lg; 14.40.Aq; 12.40.Vv

## I. INTRODUCTION

Bridging the gap between the non-perturbative and the perturbative sector of QCD is a central step toward our understanding of the strong interaction. In this context, the electro-magnetic formfactor of the charged pion  $F_\pi$  is of great interest. It is, at low momenta, extremely well reproduced by the vector dominance model. In addition, at very high momentum transfer, it is constrained by perturbative (p)QCD predictions (for a review on hadronic formfactors, see e.g. [1]). The asymptotic behavior for large space-like momentum transfer,  $Q^2 = -(p-p')^2 > 0$ , is derived in a closed form in perturbation theory [2, 3, 4],

$$Q^2 F_\pi(Q^2) \xrightarrow{Q^2 \rightarrow \infty} 16 \pi f_\pi^2 \alpha_s(Q), \quad (1)$$

where  $f_\pi = 92.4 \text{ MeV}$  denotes the pion decay constant.

A comparison of the asymptotic behavior and the experimental data determines the momentum scale where the perturbative regime of QCD is reached. Recently, the charged pion formfactor has been measured very accurately at momentum transfers  $0.6 \text{ GeV}^2 < Q^2 < 1.6 \text{ GeV}^2$  by the Jefferson Laboratory (JLAB)  $F_\pi$  collaboration [5] and lead to quite surprising results. Not only are the data at highest experimentally accessible momenta still very far from the asymptotic limit, but the trend is away from the pQCD prediction (see Fig. 1).

Moreover, it is quite remarkable that the data are still completely consistent with the vector dominance monopole fit,

$$F_{\pi, \text{mon.}}(Q^2) = \frac{M_\rho^2}{M_\rho^2 + Q^2}, \quad M_\rho = 770 \text{ MeV}, \quad (2)$$

at relatively high momentum transfer ( $Q^2 \approx 1 \text{ GeV}^2$ ). Clearly, the measurements currently undertaken at JLAB in the region  $0.5 \text{ GeV}^2 \lesssim Q^2 \lesssim 6 \text{ GeV}^2$  are very much needed and will provide information about whether the perturbative region is reached at that scale.

The charged pion formfactor has attracted a lot of attention from the theoretical side [7, 8, 9, 10, 11, 12, 13]. Despite this debate, we feel that there are still a number of open question. What are the leading non-perturbative

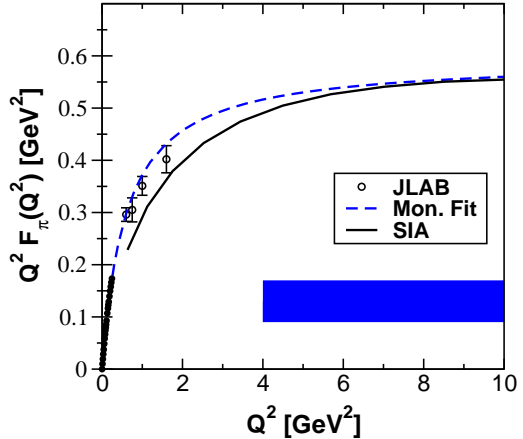


FIG. 1: The recent JLAB data for  $Q^2 F_\pi(Q^2)$  in comparison with the asymptotic pQCD prediction (thick bar, for a typical  $\alpha_s \approx 0.2 - 0.4$  in Eq. (1)), the monopole fit (dashed line), and our SIA calculation (solid line). The SIA calculation is not reliable below  $Q^2 \sim 1 \text{ GeV}^2$ . The solid circles denote the SLAC data [6].

effects responsible for the deviation from pQCD, Eq. (1), at intermediate momenta? Where can we expect the transition to pQCD, is it within experimentally accessible momentum transfers? Is there a *microscopic* explanation of the success of the monopole form? Can it be justified at so large momenta, where the vector dominance model should be inadequate?

In this work we suggest answers to these questions. In particular, we study the effects of the leading (i.e. zero-mode) interaction of light quarks with the intense classical vacuum fields (instantons) on the pion formfactor, for  $Q^2 > 1 \text{ GeV}^2$ . We show that, in this kinematic region, the pion formfactor is dominated by the interaction of quarks with a single instanton.

The pion plays a special role among the hadrons. Not only is it nearly massless (which is explained by the Goldstone theorem), but unusually compact as well. Phenomenologically, this is seen e.g., from the rather large electro-magnetic mass splittings between the charged and neutral pion. Theoretically, it was explained by studying

instanton-induced effects on the two-point correlators, see [14] for a review. In the pion channel (as well as other scalar and pseudoscalar channels) the instanton contribution to the two-point correlator can be represented by the zero-mode terms in the quark propagators, and as a result the effect is enhanced (relative to e.g., the vector or axial channels) by a factor  $1/(m^* \rho)^2$ , where  $\rho$  denotes the typical instanton size, and  $m^*$  is an effective parameter with the dimension of a mass, defined and discussed in detail in [15]. Numerically, such an enhancement factor is about 30, and parametrically it is the inverse diluteness of the instanton ensemble. Due to the presence of such a large factor, instanton-induced forces become dominant in the pion pseudoscalar correlator, starting from rather small distances. The same factor is present in the instanton contribution to the three-point function, which is related to the pion formfactor. Although, the final results we obtain are independent of the value of  $m^*$ , the window of applicability of our method does depend on it.

This feature, however, is not generically related to the pion itself and depends on the particular three-point function under investigation. For example, the enhancement is absent, when one considers the pion contribution to the axial correlator. Similarly, there is no such enhancement of the  $\gamma\gamma^*\pi^0$  neutral pion transition formfactor. The relevant instanton effects for this process are not due to (enhanced) zero modes, but are either related to non-zero mode propagators in the instanton background or to multi-instanton effects, which are suppressed by the instanton diluteness. This conclusion is nicely supported by recent CLEO measurements of this formfactor, which indeed show that the asymptotic pQCD regime is reached much earlier, at  $Q^2 \sim 2 \text{ GeV}^2$  [16].

The first calculation of the pion formfactor in the SIA was performed by Forkel and Nielsen [17], who complemented QCD sum rules by the instanton-induced contribution. In such an approach, however, a model description of the continuum of excitations with the quantum numbers of the pion is needed, in order to connect the electro-magnetic three-point function to the pion formfactor<sup>1</sup>. In order to avoid such additional model dependence, Blotz and Shuryak proposed a different approach [19], in which large-sized three-point functions obtained both from simulations in the Instanton Liquid Model (ILM) and from its spectral decomposition (which depends on the pion formfactor) were compared *directly in coordinate space*. This analysis revealed that, at large distances, the ILM results were completely consistent with the monopole fit.

In this work we follow a different approach, which is based on the mixed time-momentum representation

widely used in lattice calculations (see e.g., [20]). We show that this way it is possible to isolate the pion pole and yet make predictions in momentum space (and therefore compare directly with experiments), without any model of the continuum contribution.

This approach has several other advantages. Firstly, the model dependence is maximally reduced: Our results depend only on one dimensional parameter, the average instanton size,  $\bar{\rho} \approx 1/3 \text{ fm}$ , which was proposed many years ago [18] and checked a number of times by phenomenological studies [14] as well as lattice simulations [21, 22, 23, 24, 25]. The calculation is independent of the properties of the instanton liquid ensemble such as the instanton-instanton interaction and the instanton density. Moreover, we will argue that the physical content of the calculation is more transparent and the dynamical effects of the instantons on the propagation of the quarks can be seen naturally.

The central prediction following from our SIA calculation is shown in Fig. 1 in comparison to the recent JLAB measurements.

The main physical point of our analysis is that, if the strongly attractive 't Hooft interaction is taken into account, the asymptotic perturbative regime of the pion formfactor is reached much later than in other models, which do not include this force. Such a qualitative difference implies that the upcoming JLAB measurements will provide an important test of instanton forces in the pion. We also find the very intriguing result that the instanton contribution to the formfactor is completely consistent with the monopole form at intermediate momentum transfers,  $2 \text{ GeV}^2 < Q^2 \lesssim 10 \text{ GeV}^2$ , where the vector dominance model has no justification. It is a first microscopic study showing that all other resonances with quantum numbers of the  $\rho$  (except the  $\rho$  itself) are not seen in the pion formfactor. For large momentum transfers,  $Q^2 > 20 \text{ GeV}^2$ , our SIA breaks down, as it is necessary to increase the distances in order to isolate the pion ground state. At these needed distances, however, the correlation functions will become sensitive to multi-instanton effects.

## II. INSTANTON CONTRIBUTION TO THE FORMFACTOR

We consider the spatial Fourier transforms of the Euclidean three-point function and two-point function,

$$G_\mu(t, \mathbf{p} + \mathbf{q}; -t, \mathbf{p}) = \int d^3\mathbf{x} d^3\mathbf{y} e^{-i\mathbf{p}\cdot\mathbf{x} + i(\mathbf{p}+\mathbf{q})\cdot\mathbf{y}} \times \langle 0 | j_5(t, \mathbf{y}) J_\mu(0, \mathbf{0}) j_5^\dagger(-t, \mathbf{x}) | 0 \rangle, \quad (3)$$

$$G(2t, \mathbf{p}) = \int d^3\mathbf{x} e^{i\mathbf{p}\cdot\mathbf{x}} \langle 0 | j_5(t, \mathbf{x}) j_5^\dagger(-t, \mathbf{0}) | 0 \rangle, \quad (4)$$

where the pseudo-scalar current  $j_5(x) = \bar{u}(x) \gamma_5 d(x)$  excites states with the quantum numbers of the pion and

<sup>1</sup> Notice that in [17] Forkel and Nielsen used the numerical value for the effective parameter  $m^*$ , which was derived in the mean field approximation [18]. However later a significantly smaller value (and larger enhancement) has been derived from numerical simulations of the Instanton Liquid Model [15].

$J_\mu(0)$  denotes the electro-magnetic current operator. In the large  $t$  limit (at fixed momenta), both correlation functions are dominated by the pion pole contribution and the ratio of the three-point function to the two-point function becomes proportional to the pion form-factor [20]. In the Breit frame,  $\mathbf{p} = -\mathbf{q}/2$  and  $Q^2 = \mathbf{q}^2$ , one has simply

$$\frac{G_4(t, \mathbf{q}/2; -t, -\mathbf{q}/2)}{G(2t, \mathbf{q}/2)} \rightarrow F_\pi(Q^2). \quad (5)$$

Notice that the LHS of Eq. (5) should not depend on  $t$ , for  $t$  large enough. Below we demonstrate that, for the pion, this is achieved already for  $t \sim 0.6$  fm.

We will evaluate the LHS of Eq. (5) in the SIA. In principle, it is not obvious that such an approach is justified, as the mean Euclidean distance between two instantons in the vacuum is about 1 fm. Therefore, if  $t \sim 1$  fm, one would expect many instanton effects to play a non negligible role. However, two of the authors showed that the pion and nucleon three-point functions, evaluated in the SIA, agree with the results of numerical simulations in the instanton liquid model up to distances of the order of 1 fm [15]. Moreover, they found that the ratio of three-to two-point function is dominated by single instanton effects to even larger distances [26]. This result enables us to reliably evaluate this ratio in the SIA up to Euclidean distances of  $\sim 1.4$  fm. A possible physical interpretation of this fact is that in order for the scattered parton to recombine in the same final state (and therefore have an elastic formfactor), it is sufficient that the parton scatters off a single instanton during the process.

We expect that the main contribution to the time-momentum correlation functions comes from distances of the order of the inverse conjugate momenta,  $|\mathbf{x}| \lesssim 1/|\mathbf{p}|$  and  $|\mathbf{y}| \lesssim 1/|\mathbf{p} + \mathbf{q}|$ . Therefore, in the Breit frame and with the choice  $t \sim 0.7$  fm, one obtains that the correlation functions under consideration can be evaluated in the SIA, for momenta  $|\mathbf{q}| \gtrsim 0.6 - 1$  GeV. We note that one of the authors applied the same method to evaluate the pion and nucleon dispersion curves [27]. Agreement between the SIA calculation and experiment was found for  $t \gtrsim 0.7$  fm and  $|\mathbf{p}| \gtrsim 1$  GeV.

Having assessed the applicability of our approximation, we proceed to the calculation. The connected three-point and two-point functions are given by <sup>2</sup>

$$G_4(t, \mathbf{p} + \mathbf{q}; -t, \mathbf{p}) = (e_u - e_d) \times \int d^3\mathbf{x} d^3\mathbf{y} e^{-i\mathbf{p}\cdot\mathbf{x} + i(\mathbf{p} + \mathbf{q})\cdot\mathbf{y}} \langle \text{Tr}\{\gamma_5 S(t, \mathbf{y}; 0, \mathbf{0}) \times \gamma_4 S(0, \mathbf{0}; -t, \mathbf{x}) \gamma_5 S(-t, \mathbf{x}; t, \mathbf{y})\} \rangle, \quad (6)$$

<sup>2</sup> A discussion of the contribution from disconnected diagrams can be found in [19].

$$G(2t, \mathbf{p}) = \int d^3\mathbf{x} e^{i\mathbf{p}\cdot\mathbf{x}} \langle \text{Tr}\{\gamma_5 S(t, \mathbf{x}; -t, \mathbf{0}) \times \gamma_5 S(-t, \mathbf{0}; t, \mathbf{x})\} \rangle, \quad (7)$$

where  $S(y, x)$  denotes the quark propagator in the background of a gauge field, the  $\text{Tr}$  is over spin and color, and the brackets  $\langle \cdot \rangle$  denote the average over all gauge field configurations.

We express Eqs. (6) and (7) in terms of “wall-to-wall” (W2W) correlators, defined as the spatial Fourier transforms of the quark propagators

$$S(t', \mathbf{p}'; t, \mathbf{p}) \equiv \int d^3\mathbf{x} d^3\mathbf{y} e^{i\mathbf{p}'\cdot\mathbf{y} - i\mathbf{p}\cdot\mathbf{x}} S(y, x). \quad (8)$$

This is achieved by insertions of appropriate delta functions at each vertex

$$G_4(t, \mathbf{p} + \mathbf{q}; -t, \mathbf{p}) = \int \frac{d^3\mathbf{k}}{(2\pi)^3} \int \frac{d^3\mathbf{l}}{(2\pi)^3} \int \frac{d^3\mathbf{m}}{(2\pi)^3} \times \int \frac{d^3\mathbf{n}}{(2\pi)^3} \langle \text{Tr}\{\gamma_5 S(t, \mathbf{k}; 0, \mathbf{m} + \mathbf{n}) \gamma_4 S(0, \mathbf{m}; -t, \mathbf{l}) \times \gamma_5 S(-t, \mathbf{l} - \mathbf{p}; t, \mathbf{k} - \mathbf{p} - \mathbf{q})\} \rangle, \quad (9)$$

$$G(2t, \mathbf{p}) = \int \frac{d^3\mathbf{k}}{(2\pi)^3} \int \frac{d^3\mathbf{l}}{(2\pi)^3} \int \frac{d^3\mathbf{m}}{(2\pi)^3} \times \langle \text{Tr}\{\gamma_5 S(t, \mathbf{k}; -t, \mathbf{l}) \gamma_5 S(-t, \mathbf{m}; t, \mathbf{k} - \mathbf{p})\} \rangle. \quad (10)$$

These W2W correlation functions are completely general. Their graphical representation, as an example for the three-point function, Eq. (9), is given in Fig. 2 (A).

A model dependence is introduced, when we evaluate the gauge field average in the SIA. This is achieved by taking the quark propagators in the background of an instanton and averaging over the collective coordinates (instanton position, size and color orientation). The integration over the color orientation is trivial, while the integration over the instanton size is weighted by a distribution function. We use a distribution for the instanton size which takes into account the small-size limit. The latter has been calculated by 't Hooft, by considering perturbative fluctuations around the instanton solution [28, 29]. For large-sized instantons, however, the distribution has to be cut off. We use a Fermi distribution function to account for the suppression of large-sized instantons, where we fit the width and the mean instanton size to lattice QCD results (for a summary on lattice QCD results, see e.g., Negele [30]). This leaves for the single instanton density

$$n(\rho) = \bar{n} d_{\text{t Hooft}}(\rho) \frac{1}{\exp((\rho - \bar{\rho})/\sigma) + 1}, \quad (11)$$

where  $\bar{n}$  denotes the average instanton density and the QCD small-size limit is given by 't Hooft

$$d_{\text{t Hooft}}(\rho) \sim \rho^{N_f - 5} \beta_1(\rho)^{2N_c} \times \exp\{-\beta_2(\rho) + (2N_c - \frac{b'}{2b}) \frac{b'}{2b \beta_1(\rho)} \ln(\beta_1(\rho))\}. \quad (12)$$

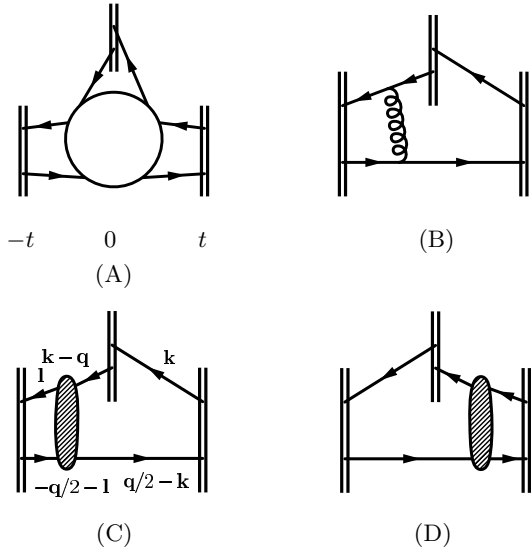


FIG. 2: (A): Graphical representation of the W2W three point function, Eq. (9). The double lined “walls” correspond to the spatial Fourier integration. (B): A particular diagram contributing to (A), in lowest order pQCD. (C) and (D): The leading non-perturbative contributions to (A) in the SIA. The dashed ellipse denotes the quark (zero-mode) ’t Hooft interaction. Note that the momentum integrations in Eqs. (9) and (10) ensure locality at the walls and the gauge invariance of the calculation.

Here,  $\beta_1(\rho)$  and  $\beta_2(\rho)$  denote the one and two-loop beta functions<sup>3</sup>,

$$\beta_1(\rho) = -b \ln(\rho \Lambda_{PV}), \quad (13)$$

$$\beta_2(\rho) = \beta_1(\rho) + \frac{b'}{2b} \ln(2 \ln(1/\rho \Lambda_{PV})), \quad (14)$$

$$b = \frac{11}{3} N_c - \frac{2}{3} N_f, \quad (15)$$

$$b' = \frac{34}{3} N_c^2 - \frac{13}{3} N_c N_f + \frac{N_f}{N_c}. \quad (16)$$

For our analysis, we use a parameterization, which summarizes recent lattice QCD results [30],  $\bar{\rho} = 0.37$  fm and  $\sigma = 0.15$  fm. We will also contrast this size density to a much simpler model proposed by Shuryak [18],  $n(\rho) = \bar{n} \delta(\rho - \bar{\rho})$ , where  $\bar{\rho} = 1/3$  fm.

The quark propagator in the field of an instanton was evaluated exactly in singular gauge [31] and consists of a zero-mode and a non zero-mode part,

$$S^I(x, y) = S_{zm}^I(x, y) + S_{nzm}^I(x, y). \quad (17)$$

The expression for  $S_{nzm}^I$  is quite involved. However, at small distances,  $|x - y| \ll \rho$ , and if the instanton is far

away,  $|x - z|, |y - z| \gg \rho$ , the non zero-mode propagator reduces to the free one. For this reason, most calculations are carried out in the zero-mode approximation (ZMA)<sup>4</sup>, in which one approximates the non zero-mode part with a free massless quark propagator,

$$S^I(x, y) \approx S_0(x, y) + S_{zm}^I(x, y). \quad (18)$$

Let us discuss the accuracy of the ZMA for our calculation. We recall that, in the momentum range of interest, the contributing point-to-point correlators in Eqs. (3) and (4), are  $\sim 1$  fm long. It is therefore sufficient to access the accuracy of the ZMA for our point-to-point correlators at those distances. In [15], two of the authors have evaluated several three- and two-point functions in the SIA with ZMA and compared them with the results of numerical simulations in the instanton liquid model (where non-zero mode effects are taken into account). Very good agreement was observed at distances relevant for our calculation. This result could either imply that multi-instanton and non-zero mode effects are individually small at that scale, or that both effects are not quite small, but that they happen to cancel.

In this approximation, the non-perturbative contributions to Eq. (9) are represented in Figs. 2 (C) and (D) and are straightforward, once the free and zero-mode W2W quark propagators are evaluated.

The massless free W2W quark propagator is given by

$$S_0(t', \mathbf{p}'; t, \mathbf{p}) = (2\pi)^3 \delta^{(3)}(\mathbf{p}' - \mathbf{p}) \frac{e^{-|\mathbf{p}||t' - t|}}{2} u_\mu \gamma_\mu, \quad (19)$$

where  $u_4 = 1$  and  $u_l = i p_l / |\mathbf{p}|$ , for  $l = 1, 2, 3$ . We note that the free W2W propagator is proportional to a delta function due to momentum conservation. The free contribution to  $G_4$  and  $G$  are then given by

$$G_4^{(\text{free})}(t, \mathbf{p} + \mathbf{q}; -t, \mathbf{p}) = -\frac{3}{2} \int \frac{d^3 \mathbf{k}}{(2\pi)^3} \left( \frac{\mathbf{k} \cdot (\mathbf{k} - \mathbf{q})}{|\mathbf{k}| |\mathbf{k} - \mathbf{q}|} - \frac{\mathbf{k} \cdot (\mathbf{k} - \mathbf{p} - \mathbf{q})}{|\mathbf{k}| |\mathbf{k} - \mathbf{p} - \mathbf{q}|} - \frac{(\mathbf{k} - \mathbf{q}) \cdot (\mathbf{k} - \mathbf{p} - \mathbf{q})}{|\mathbf{k} - \mathbf{q}| |\mathbf{k} - \mathbf{p} - \mathbf{q}|} + 1 \right) e^{-t(|\mathbf{k}| + |\mathbf{k} - \mathbf{q}| + 2|\mathbf{k} - \mathbf{p} - \mathbf{q}|)}, \quad (20)$$

$$G^{(\text{free})}(2t, \mathbf{p}) = 3 \int \frac{d^3 \mathbf{k}}{(2\pi)^3} \left( \frac{\mathbf{k} \cdot (\mathbf{k} - \mathbf{p})}{|\mathbf{k}| |\mathbf{k} - \mathbf{p}|} - 1 \right) e^{-2t(|\mathbf{k}| + |\mathbf{k} - \mathbf{p}|)}. \quad (21)$$

The free W2W two-point function can be further simplified,

$$G^{(\text{free})}(2t, \mathbf{p}) = \frac{3}{(2\pi)^2} \frac{1 + 2t |\mathbf{p}|}{(2t)^3} e^{-2t |\mathbf{p}|}. \quad (22)$$

<sup>3</sup> This result was carried out in the Pauli-Villars regularization scheme and  $\Lambda_{PV}$  is the corresponding scale parameter. We use  $\Lambda_{PV} = 250$  MeV.

<sup>4</sup> We note that, at large distances ( $|x - y| \gg \rho$ ), the zero-mode approximation gives the same correlation functions as the ’t Hooft Lagrangian.

Next, we calculate the zero-mode W2W quark propagator. Since we are eventually interested in a gauge invariant quantity, and we are working in the SIA, we can use the instanton solution in regular gauge<sup>5</sup>, where we find the simple result:

$$S_{zm}^{I(A)}(t', \mathbf{p}'; t, \mathbf{p}) = \frac{2\rho^2}{m^*} f(t', \mathbf{p}'; t, \mathbf{p}) \mathbf{W}^{I(A)}, \quad (23)$$

$$\begin{aligned} f(t', \mathbf{p}'; t, \mathbf{p}) &\equiv e^{i(\mathbf{p}' - \mathbf{p}) \cdot \mathbf{z}} K_0(|\mathbf{p}'| \sqrt{(t' - z_4)^2 + \rho^2}) \\ &\quad \times K_0(|\mathbf{p}| \sqrt{(t - z_4)^2 + \rho^2}), \end{aligned} \quad (24)$$

$$\mathbf{W}^{I(A)} \equiv \gamma_\mu \gamma_\nu \frac{1 \pm \gamma_5}{2} \tau_\mu^\mp \tau_\nu^\pm, \quad (25)$$

where  $z_\mu = (\mathbf{z}, z_4)$  denotes the instanton position,  $m^*$  is the effective parameter encoding many-instanton effects defined in [15] and  $\tau_\mu^\pm = (\tau, \mp i)$  are color matrices. We remark that the spatial instanton position appears only coupled to the quark momentum transfer in the background of the instanton field. This is intuitive: if the instanton is far away from the quark, there should be little momentum transfer. Due to this fact, the integration over the spatial instanton position leads to an overall momentum conserving delta function. As expected, the momentum conservation in the SIA is a consequence of the translational invariance of the spatial instanton position. Moreover, the modified Bessel functions exponentially suppress momentum transfers much larger than the inverse size of the instanton,  $1/\rho$ . This implies that large momentum transfers are driven by small instantons and directly probe the small-size limit of the 't Hooft measure for the tunneling amplitude. This argument holds for all W2W correlation functions evaluated in the SIA and was applied by one of the authors to the pion and nucleon correlators [27]. It was shown that at sufficiently large momenta, all the model-dependence in such a semi-classical approach is removed, and the physical observables can be expressed in terms of  $\Lambda_{\text{QCD}}$ . We shall similarly study at what momentum transfer the pion formfactor becomes sensitive to the small-sized instantons only.

The explicit evaluations of the zero-mode contributions, Figs. 2 (C) and (D), lead to

$$\begin{aligned} G_{4zm}^{(C)} &= \int_0^\infty d\rho \int_{-\infty}^\infty dz_4 \int \frac{d^3\mathbf{k}}{(2\pi)^3} \int \frac{d^3\mathbf{l}}{(2\pi)^3} n(\rho) \\ &\quad \times \frac{512\rho^4}{m^{*2}} e^{-|\mathbf{k}|t} K_0(|\mathbf{k} - \mathbf{q}| \xi(z_4)) K_0(|\mathbf{q}/2 - \mathbf{k}| \xi(z_4 - t)) \\ &\quad \times K_0(|-\mathbf{l} - \mathbf{q}/2| \xi(z_4 + t)) K_0(|\mathbf{l}| \xi(z_4 + t)), \end{aligned} \quad (26)$$

$$\begin{aligned} G_{4zm}^{(D)} &= \int_0^\infty d\rho \int_{-\infty}^\infty dz_4 \int \frac{d^3\mathbf{k}}{(2\pi)^3} \int \frac{d^3\mathbf{l}}{(2\pi)^3} n(\rho) \\ &\quad \times \frac{512\rho^4}{m^{*2}} K_0(|\mathbf{k}| \xi(z_4 - t)) K_0(|\mathbf{q}/2 - \mathbf{k}| \xi(z_4 - t)) e^{-|\mathbf{l}|t} \\ &\quad \times K_0(|-\mathbf{l} - \mathbf{q}/2| \xi(z_4 + t)) K_0(|\mathbf{l} + \mathbf{q}| \xi(z_4)), \end{aligned} \quad (27)$$

where  $\xi(x) \equiv \sqrt{x^2 + \rho^2}$ . We have labeled the momenta, flowing from left to right, for the case of Eq. (26) in Fig. 2 (C). We note that the presence of the (non-perturbative) instanton-induced interaction results in an integration over the momentum exchanged by the quarks through the instanton, similar to the presence of perturbative gluon exchanges leading to loop integrals, Fig. 2 (B). This analogy still holds when multi-instanton effects are taken into account: each instanton gives an additional ‘loop’ integral over the instanton induced momentum transfer. Furthermore, we read off the ‘Feynman rules’: each free quark propagator contributes an exponential and each zero-mode a modified Bessel function. Combined, the W2W three-point function, Eq (9), in the SIA reads

$$G_4 = G_4^{(\text{free})} + G_{4zm}^{(C)} + G_{4zm}^{(D)}. \quad (28)$$

Time reversal invariance imposes that the contributions from Figs. 2 (C) and (D) are equal, as can be seen from Eqs. (26) and (27) by substituting  $t \rightarrow -t$  and  $\mathbf{q} \rightarrow -\mathbf{q}$  (recall the absolute value in the exponential of the free W2W propagator, Eq. (19)). Finally, the W2W two-point function, Eq. (10), in the SIA, is given by

$$\begin{aligned} G_{zm} &= \int_0^\infty d\rho \int_{-\infty}^\infty dz_4 n(\rho) \frac{\rho^4}{4m^{*2}} e^{-|\mathbf{q}|/2} (\xi(z_4 - 2t) + \xi(z_4)) \\ &\quad \times \frac{(1 + |\mathbf{q}| \xi(z_4 - 2t)/2)}{\xi(z_4 - 2t)^3} \frac{(1 + |\mathbf{q}| \xi(z_4)/2)}{\xi(z_4)^3}, \end{aligned} \quad (29)$$

and analogously

$$G = G^{(\text{free})} + G_{zm}. \quad (30)$$

The pion formfactor is now readily obtained by means of Eq. (5). At the distances we are considering ( $t = 0.7 \text{ fm}$ ), the free contribution to the correlation functions,  $G_4^{(\text{free})}$  and  $G^{(\text{free})}$ , are at most 30% corrections (at  $|\mathbf{q}| = 5 \text{ GeV}$ ) to the zero-mode three- and two-point functions. This can be seen by evaluating e.g., the zero-mode two-point function for large  $|\mathbf{q}|$ :

$$G_{zm} = \int_0^\infty d\rho \frac{n(\rho) \rho^4}{16m^{*2} \rho} \sqrt{\frac{2\pi}{\xi^5(t)}} |\mathbf{q}|^{3/2} e^{-|\mathbf{q}| \xi(t)}, \quad (31)$$

by a saddle point analysis of the  $z_4$  integration. In comparison to the free contribution, Eq. (22), this leads to a 30% correction at  $|\mathbf{q}| = 5 \text{ GeV}$ , for standard values of the average instanton density  $\bar{n} = 1 \text{ fm}^{-4}$  and the quark effective mass  $m^* = 70 \text{ MeV}$ . We consider such a correction

<sup>5</sup> When one considers many instanton effects, the use of the singular gauge is obligatory, as one desires the topological charge to be localized. In singular gauge, however, the expression of the zero-mode W2W quark propagator is more complicated.

to be the edge of the window we work in<sup>6</sup>. Therefore, we may approximate the formfactor by<sup>7</sup>

$$\begin{aligned} & \frac{G_4^{(\text{free})}(t, \frac{\mathbf{q}}{2}; -t, -\frac{\mathbf{q}}{2}) + G_{4zm}^{(C)+(D)}(t, \frac{\mathbf{q}}{2}; -t, -\frac{\mathbf{q}}{2})}{G^{(\text{free})}(2t, \mathbf{q}/2) + G_{zm}(2t, \mathbf{q}/2)} \\ & \simeq \frac{G_{4zm}^{(C)+(D)}(t, \frac{\mathbf{q}}{2}; -t, -\frac{\mathbf{q}}{2})}{G_{zm}(2t, \mathbf{q}/2)} \rightarrow F_\pi(Q^2). \end{aligned} \quad (32)$$

Consequently, the effective parameter  $m^*$  and the average instanton density  $\bar{n}$ , which are multi-instanton induced model parameters, are irrelevant for the pion formfactor at intermediate momentum transfer. We stress that, in the approach presented here, we do not need to evaluate the pion wave function, since we obtain directly the relevant Green functions from the SIA. In other words, the pion wave function is implicitly included in our calculation through the large time extraction of the pion pole.

### III. NUMERICAL RESULTS

Before comparing our results to the experimental data, we check that the ratio of the zero-mode three-point to two-point function, Eq. (32), does not depend on the distance  $t$ , which ensures that the pion pole contribution has been successfully isolated. For this purpose, we show

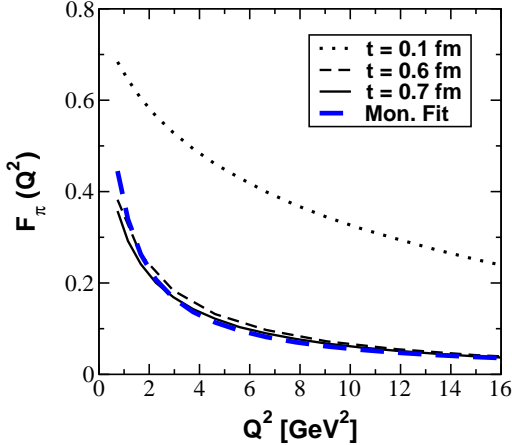


FIG. 3: The ratio of three- to two-point function, Eq. (32), evaluated in the SIA for different values of  $t$  and for simplicity a delta function distribution at  $\bar{\rho} = 1/3$  fm. At  $t > 0.5$  fm our results are  $t$  independent.

this ratio for several distances  $t$  in Fig. 3. We find that the pion pole contribution dominates for  $t > 0.5$  fm, in agreement with [14, 27].

Our central result for the pion formfactor is plotted in Fig. 1 in comparison to the JLAB data and the monopole formfactor fitted to the low  $Q^2$  data. We observe that the SIA prediction agrees with the recent JLAB measurements. In addition, it is completely consistent with the monopole form in the kinematic region accessible to JLAB. These results complement the analysis of Blotz and Shuryak [19], where the same agreement was found at small momentum transfer. Upcoming measurements at JLAB will be able to test the single instanton prediction as the microscopic mechanism at intermediate momentum transfer.

We find that the instanton contribution remains well above the pQCD scale set by Eq. (1) throughout the experimental region under investigation at JLAB,  $Q^2 \lesssim 6$  GeV $^2$ .

As the momentum is increased, one requires larger times in order to isolate the pion pole from the higher excitations. In sum-rule approaches, contributions from the continuum are obtained from the free and perturbative gluon exchange correlation functions, e.g., Fig. 2 (B). Perturbative contributions will never develop a pion pole. Indeed, we observed that the free correlators,  $G_4^{(\text{free})}$  and  $G^{(\text{free})}$ , become non negligible for  $|\mathbf{q}| \gtrsim 4 - 5$  GeV. The presence of such continuum contributions destroys the time-independence of the ratio of three- to two-point functions around  $t \sim 0.6$  fm, shown in Fig. 3, and hence the method can no longer be used.

In principle, one could extend the range of validity of our approach by increasing the time. However we recall that, when  $t$  becomes larger, multi-instanton effects are significant and the SIA breaks down. We conclude that our approach is not applicable to the study of the high momentum transfer region,  $Q^2 > 20$  GeV $^2$ .

Let us now discuss, how one can get the transition to the pQCD limit from instantons. For large momentum transfer, where counting rules and factorization are justified, the evaluation of the formfactor requires non-perturbative information, encoded in the pion wave func-

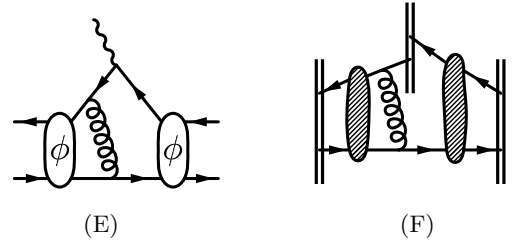


FIG. 4: (E): Diagram contributing to the formfactor at asymptotic momentum transfer in pQCD. The blobs denote the pion wave functions  $\phi$ . (F) A leading order multi-instanton contribution to the W2W three-point correlator responsible for the transition toward the pQCD result.

<sup>6</sup> Note, however, that similar corrections appear in the numerator and the denominator, and thus the real accuracy of the formfactor can actually be better.

<sup>7</sup> We note that the free correlators do not have a pion pole. They are the leading order  $\mathcal{O}(\alpha_s^0)$  continuum contributions. The relevance of these terms at higher momentum transfer demands larger times  $t$ . As discussed, however, then the SIA breaks down.

tion  $\phi$ , in addition to pQCD diagrams. This is shown diagrammatically in Fig. 4 (E). In the instanton liquid model, the pion is bound because the quark and anti-quark feel a strong attraction from instantons. As we argued, at large momentum transfers, one has to incorporate multi-instanton effects in order to isolate the pion pole and the pion wave function. For example, we give a leading order multi-instanton diagram relevant in the asymptotic limit in Fig. 4 (F).

Since the pion formfactor may experimentally be rather accurately measured, it is instructive to ask whether such data may shed some light on the instanton size distribution. In Fig. 5, we have plotted the results of our theoretical predictions for  $Q^2 F_\pi(Q^2)$  obtained for different cases of  $n(\rho)$ . We contrast the simplest size distribution [18],  $n(\rho) \sim \delta(\rho - 1/3 \text{ fm})$ , to the results obtained from a lattice QCD parameterization. We notice that the presence of tails in the size distribution introduces only small corrections to the formfactor. Therefore, we conclude that the simplest distribution  $n(\rho) \sim \delta(\rho - 1/3 \text{ fm})$  indeed captures the relevant features for the pion formfactor at intermediate momentum transfer. We observe that our result becomes closer to the perturbative limit, if the average instanton size is larger or possibly if there is an asymmetric tail toward larger-sized instantons in the distribution.

Next, we compare the results from distributions which have the same small-size limit, but cut off at different instanton sizes,  $\bar{\rho} = 0.37 \text{ fm}$  and  $0.47 \text{ fm}$ . We observe that, throughout the entire kinematic region we have considered, our predictions are quite sensitive to the average instanton size. This implies that the asymptotic region, where the pion formfactor probes the small-size 't Hooft behavior, is not reached within the window, where our

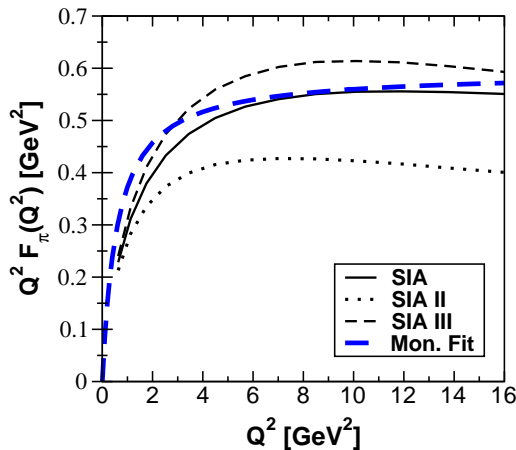


FIG. 5: The dependence of the pion formfactor  $Q^2 F_\pi(Q^2)$  on the instanton size distribution. The SIA (solid) curve represents a small-size 't Hooft distribution with a Fermi distribution cutoff and lattice QCD parameters. The SIA II (dotted) curve has a different mean instanton size  $\bar{\rho} = 0.47 \text{ fm}$  (same width) and the SIA III (dashed) curve is obtained with the simplest delta distribution  $n(\rho) = \bar{n} \delta(\rho - 1/3 \text{ fm})$ .

approach is justified.

Summarizing, we have shown that the presence of enhanced instanton-induced forces constitutes a large and clearly dominant contribution to the charged pion formfactor. The latter is so large that the perturbative regime will not be reached experimentally. This nicely contrasts the situation for the  $\gamma\gamma^*\pi^0$  neutral pion transition formfactor, where the asymptotic pQCD regime is reached much earlier, at  $Q^2 \sim 2 \text{ GeV}^2$  [16]. This striking difference is explained by instanton arguments as well, because the two corresponding three-point functions have a different chiral structure. Physically, this is the same reason why the vector and axial channels have a rather strong "Zweig" rule, forbidding flavor mixing, while for the pseudoscalars such a mixing is very strong.

#### IV. CONCLUSIONS

We have presented the first calculation of the instanton contribution to the charged pion electro-magnetic formfactor in the momentum range  $Q^2 > 1 \text{ GeV}^2$ . Technically, it is based on the ratio of three- to two-point correlators, in which the enhancement comes from the zero-mode quark W2W propagators. Because it is based on a representation in momentum space, the framework developed presents several quite direct analogies with ordinary perturbative calculus.

Our calculation shows that, when the non-perturbative instanton-induced forces are taken into account, the charged pion formfactor remains much larger than the asymptotic perturbative prediction, throughout the entire experimentally accessible region of JLAB. This result is in contrast to other model calculations, which do not include such a force [7, 8, 9, 10, 11, 12, 13]. Clearly, the upcoming JLAB measurements will provide a unique opportunity to test the role played by the instanton-induced 't Hooft interaction in hadronic physics.

Moreover, we found that the SIA prediction coincides with the monopole form up to  $Q^2 \sim 10 \text{ GeV}^2$ . We emphasize that this does not represent a test of the validity of our model, since the monopole fit is a phenomenological parametrization exclusively of the low energy data. Nevertheless, such an agreement is interesting, because it suggests that the widely used vector dominance model for the pion is in fact a dynamic property of the QCD vacuum, and that its validity extends into the intermediate momentum regime.

We finally studied whether our results depend on the details of the instanton size distribution. We found that the pion formfactor is determined by the average instanton size up to rather large  $Q^2$  and is insensitive to the details of the size distributions.

In addition, an application of the same method to the analysis of the proton electric formfactor has been carried out and leads to a dipole formfactor at intermediate momentum transfers [32].

## Acknowledgments

We would like to thank Thomas Schäfer and George Sterman for interesting discussions. The work is sup-

ported by the US DOE grant No. DE-FG02-88ER40388.

---

[1] G. Sterman and P. Stoler, *Annu. Rev. Nucl. Part. Sci.* **47** (1997) 193.

[2] V.L. Chernyak, V.G. Serbo, and A.R. Zhitnitsky, *JETP Lett.* **26** (1977) 594.

[3] A.V. Efremov and A.V. Radyushkin, *Phys. Lett.* **B94** (1980) 245.

[4] G.P. Lepage and S.J. Brodsky, *Phys. Rev.* **D22** (1980) 2180.

[5] J. Volmer *et al.* [The Jefferson Laboratory  $F_\pi$  Collaboration], *Phys. Rev. Lett.* **86** (2001) 1713.

[6] S.R. Amendolia *et al.*, *Nucl. Phys.* **B277** (1986) 168.

[7] V.A. Nesterenko and A.V. Radyushkin, *Phys. Lett.* **B115** (1982) 410; A.V. Radyushkin, *Nucl. Phys.* **A532** (1991) 141.

[8] V.L. Chernyak and A.R. Zhitnitsky, *Phys. Rept.* **112** (1984) 173.

[9] R. Jacob and P. Kroll, *Phys. Lett.* **B315** (1993) 463.

[10] F. Cardarelli *et al.*, *Phys. Lett.* **B332** (1994) 1; *Phys. Lett.* **B357** (1995) 267.

[11] H. Ito, W.W. Buck, and F. Gross, *Phys. Rev.* **C45** (1992) 1918.

[12] P. Maris and C.D. Roberts, *Phys. Rev.* **C58** (1998) 3659.

[13] P. Maris and P.C. Tandy, *Phys. Rev.* **C62** (2000) 055204.

[14] T. Schaefer and E.V. Shuryak, *Rev. Mod. Phys.* **70** (1998) 323.

[15] P. Faccioli and E.V. Shuryak, *Phys. Rev.* **D64** (2001) 114020.

[16] J. Gronberg *et al.*, *Phys. Rev.* **D57** (1998) 33.

[17] H. Forkel and M. Nielsen, *Phys. Lett.* **B345** (1997) 55.

[18] E.V. Shuryak, *Nucl. Phys.* **B214** (1982) 237.

[19] A. Blotz and E.V. Shuryak, *Phys. Rev.* **D55** (1997) 4055.

[20] T. Draper, R.M. Woloshyn, W. Wilcox, and K.F. Liu, *Nucl. Phys.* **B318** (1989) 319.

[21] D.A. Smith and M.J. Teper, *Phys. Rev.* **D58** (1998) 014505.

[22] A. Hasenfratz and C. Nieter, *Phys. Lett.* **B439** (1998) 366.

[23] P. de Forcrand, M. Garcia Perez, J.E. Hetrick and I.O. Stamatescu, [hep-lat/9802017](#).

[24] M.C. Chu, J.M. Grandy, S. Huang, and J.W. Negele, *Phys. Rev.* **D49** (1994) 6039.

[25] T.L. Ivanenko and J.W. Negele, *Nucl. Phys. Proc. Suppl.* **63** (1998) 504.

[26] P. Faccioli and E.V. Shuryak, *Phys. Rev.* **D65** (2002) 076002.

[27] P. Faccioli, *Phys. Rev.* **D65** (2002) 094014.

[28] G. 't Hooft, *Phys. Rev. Lett.* **37** (1976) 8.

[29] G. 't Hooft, *Phys. Rev.* **D14** (1976) 3432.

[30] J.W. Negele, *Nucl. Phys. Proc. Suppl.* **73** (1999) 92.

[31] L.S. Brown, R.D. Carlitz, D.B. Craemer, and C. Lee, *Phys. Rev.* **D17** (1978) 1583.

[32] P. Faccioli, A. Schwenk, and E.V. Shuryak, [hep-ph/0205307](#).